Research Article

José Manuel Sandoval-Díaz, Francisco Javier Rivera-Gálvez, Marta Fernández-García, and Carlos Federico Jasso-Gastinel*

Redox initiation in semicontinuous polymerization to search for specific mechanical properties of copolymers

https://doi.org/10.1515/epoly-2020-0065
received February 25, 2020; accepted July 20, 2020

Abstract: In this work, for a semicontinuous emulsion polymerization reaction, it is shown that using a redox initiation system at 40°C, substantial modifications in copolymer chain composition with conversion can be easily obtained. To test controllable trajectories for comonomer feeding, linear and parabolic profiles were chosen to get different types of chain composition variations for the 50/50 w/w styrene/*n*-butyl acrylate system. For the "forced composition copolymers," the molecular weight averages and distribution were obtained by size exclusion chromatography. The composition along conversion was followed by proton nuclear magnetic resonance to determine the weight composition distribution (WCD) of the copolymer chains. Mechanodynamic (dynamic-mechanical analysis), tensile, and hardness tests exhibited consistent results depending on the WCD that outcomes from the respective feeding profile. The results confirm that this methodology is of great potential for industrial applications when looking for synergy in copolymer properties, and low-cost processes.

Keywords: redox initiation, semicontinuous emulsion polymerization, comonomer feed profiles, gradient composition, mechanical properties

*** Corresponding author: Carlos Federico Jasso-Gastinel,** Chemical Engineering Department, Universidad de Guadalajara, Blvd. Gral. Marcelino García Barragán, 1421, Guadalajara 44430, Jalisco, Mexico, e-mail: carlos.jasso@cucei.udg.mx
José Manuel Sandoval-Díaz, Francisco Javier Rivera-Gálvez: Chemical Engineering Department, Universidad de Guadalajara, Blvd. Gral. Marcelino García Barragán, 1421, Guadalajara 44430, Jalisco, Mexico
Marta Fernández-García: Chemistry and Properties of Polymeric Materials Department, Institute of Polymer Science and Technology, ICTP-CSIC, Juan de la Cierva, 3, 28006, Madrid, Spain

1 Introduction

Searching for copolymer properties improvement (comparing with statistical copolymers), alternate or periodical copolymers can only be formed in a few cases because of the dependency on the comonomer relative reactivities, and their properties show the tendency toward weighted values of the homopolymers, depending on the global composition. That is, they do not allow a synergistic contribution of the components, because there are no chains that are rich in one of these components (e.g. gradient composition) or long segments of one of them in a chain (e.g. block composition) within the polymer bulk. Improved results have been obtained with block or graft copolymers of uniform composition, varying size and number of blocks, or graft density for example (1,2). However, their industrial production has been limited due to reaction complexities, as well as the difficulties to obtain well-defined structures (affecting the desired properties), and/or the long reaction times, along with the use of costly catalysts or high synthesis temperature, which increases energy costs (3).

For these reasons, the development of new synthesis strategies to make copolymeric materials has continued, focusing researchers on effective ways to improve the properties' contribution of the two components to extend and diversify their engineering applications (4,5). In this way, different types of reactions and processes as well as comonomer addition techniques have evolved to optimize their properties and/or production costs (6,7).

To work in that direction, using free-radical polymerization, a significant change in properties has been accomplished forming composition gradients across one dimension in solid polymers (e.g. through the thickness) preparing sequential interpenetrating polymer networks (8,9). Such an idea has been adapted to copolymers forming gradients in chains composition as the chains are formed along with the reaction but keeping the

planned global composition. In this way, a distribution of composition for the copolymer chains is formed within the polymer bulk, and its properties are determined by the whole weight composition distribution (WCD). Such gradient principle has been reported for copolymers "forcing their composition" to make forced composition copolymers (FCC) through the reaction time by variations in the feed composition of the comonomers using semicontinuous emulsion polymerization in free-radical polymerization (10).

With the feeding technique, the instantaneous copolymer composition can be guided by looking for chains that are rich in one (A) of the two components at the beginning, and as the conversion advances, chains rich in the other component (B) can be formed. In this situation, the chains that are rich in "A," enhance the "A" contribution, and an equivalent enhanced effect can be obtained with the "B" component. The rationalization of the properties enhancement attained with the gradient feeding technique explained here also applies to changes in composition within one molecule for reactions carried out by reversible deactivation radical polymerization that has been developing in this century (11,12). In fact, for the development of this type of reaction, some efforts on reaction modeling have been reported for homogeneous systems (solution polymerization) in a semicontinuous process, varying comonomer composition in continuous form with a metering pump. The modeling scheme was satisfactory with the styrene/*n*-butyl acrylate system up to molecular weights of 25,000 using different types of feeding strategies (13). For faster reactions that are more useful using emulsion reactions, several schemes have been experimentally reported for copolymers (14), but the modeling for heterogeneous systems becomes too complicated. Recent studies report some advances but only for homopolymers, using suspension (15) or miniemulsion (16).

In the same manner, there are no successful reports for kinetic mechanism modeling in traditional free radical copolymerization for heterogeneous reactions, to model composition variations along conversion as the feed composition varies. Nevertheless, a simplified model using three parameters (apparent reactivities, feed composition, and conversion curve) to follow the sequence distribution and cumulative composition tracing has been satisfactorily developed (17). This has been possible at 80°C using potassium persulfate as initiator. In summary, more efforts are required in both types of reactions to advance in kinetic modeling. The panorama is even worse for redox reactions in free-radical copolymerization (as is the case for this work) where is very difficult to measure the relative reactivities due to the fast rate of radicals generation and copolymer conversion.

Regarding properties synergism for the "A" and "B" components, it has been accomplished in polymer systems of two and three components, achieving their interaction at micro or nanolevel (10,18). The gradual change in polymer composition along the reaction promoted the formation of a polymer bulk of chains with rich domains of each component and allowed the strong interactions toward properties optimization. In this way, a high Young modulus combined with high toughness was obtained with an adequate WCD (10).

Nevertheless, FCC synthesis has been performed using thermal decomposition initiators at 70°C, to get a convenient radicals generation rate, and be able to maintain an adequate polymerization rate for moderate or long reaction times (4–12 h), to then avoid an excessive monomer accumulation in the polymerization locus (18–20). This initiation mode usually requires long times for the polymerization process, which involves high energy costs. Such a situation is not attractive to apply the method at the industrial level. To decrease reaction time and temperature, redox initiators can be proposed for this process; they are widely used in industry because they allow a higher rate of radical formation at lower temperatures (21–23). Consequently, the combination of the FCC synthesis methodology with the use of redox initiators is proposed here not only to expand the monomers range (24,25) but also to simplify the formation of copolymers that can fulfill the requirements for rigid, semirigid, or elastic materials pertaining to the thermoplastics area (i.e. that can be reprocessed or recycled).

For this study, four different FCC are synthesized using a 50/50 w/w styrene/*n*-butyl acrylate (S/BA) chemical system, by means of a semicontinuous free-radical emulsion polymerization with redox initiators. For the feeding profiles, two different types of pairs are used. For each type, a basic profile is proposed, and a small change is used keeping the same basic pattern, trying to promote small changes in a composition histogram, to then generate changes in mechanical properties. A statistical copolymer (SC) with the same global compositions is used as reference material. Copolymer conversion and composition along the reaction are, respectively, followed by gravimetry and proton nuclear magnetic resonance (^{1}H-NMR) to construct the composition histogram. Mechanical properties are evaluated by static (tensile and hardness) and dynamic (storage and loss modulus as a function of temperature) measurements.

For the results, a wide variety of mechanical properties (e.g. to obtain a wide range of values for Young

modulus, as well as deformation and toughness/energy dissipation capacity) is expected, having as main aim to demonstrate that the synthesis of copolymers with a predetermined combination of properties is feasible using redox initiation in a semicontinuous polymerization process.

2 Experimental

2.1 Materials

Styrene (S) and *n*-butyl acrylate (BA) monomers (both from Sigma-Aldrich, purity ≥ 99%) were disinhibited with ionic exchange resins to remove methyl ester hydroquinone from BA and 4-*tert*-butylcathechol from S (both from Sigma-Aldrich). As a surfactant, sodium dodecylsulfate (SDS; Sigma-Aldrich, purity > 98%) was used. Potassium persulfate (KPS) was used as a thermal initiator (for seed synthesis); ammonium persulfate (APS) and sodium bisulfite (SB) (both from Sigma Aldrich, purity ≥ 99%) were used as the redox initiation system for the synthesis of the FCC. Sodium bicarbonate (Sb) (Arm and Hammer) was used as a pH buffer during all reactions. In all polymerization reactions, distilled water (Selectro Pura) and nitrogen gas (Infra S.A., to purge air from the reaction system and preserve an inert atmosphere) were used.

2.2 Synthesis

2.2.1 Polymer seed (PS)

About 1,400 g of distilled water was charged to a 4 L glass reactor at 70 ± 2°C to be stirred at 400 ± 5 rpm. Then, a solution of 300 mL of distilled water with 10 g of SDS and 500 g of S was added to the reactor. The system was purged with nitrogen gas for one hour before the reaction started, maintaining an inert atmosphere during the whole polymerization. To start the reaction, a 300 mL water solution of 10.0 g of KPS and 10.0 g of SB was added. The reaction conditions were maintained for 2 h to maximize conversion and obtain the polystyrene (PS) particles.

2.2.2 SC

The synthesis preparation started with the addition of 900 g of distilled water to a glass reactor; the system was heated up to 40 ± 2°C under stirring (400 ± 5 rpm); then, 300 mL of a water solution containing 10 g of SDS was added to the reactor, purging the system with nitrogen for 1 h to ensure an inert atmosphere (maintaining nitrogen flow during all the reaction). About 250 g of S and 250 g of BA previously mixed were then added to the reactor followed up by 400 mL of a water solution containing 25 g APS, and then 400 mL of a water solution containing 25 g of SB was added directly to the system to start the reaction. The conditions in the reaction system were kept for 4 h to maximize conversion (followed by gravimetry).

2.2.3 FCC

All the reactions were carried out at 40 ± 2°C in a 4 L glass reactor, stirring the system at 400 ± 5 rpm and keeping the reaction conditions for 4 h to maximize conversion (followed by gravimetry), purging the system with nitrogen gas as in the former reactions. Approximately 20 wt% of the solid copolymer was obtained at the end of every reaction. Four FCC were synthesized by means of a seeded semicontinuous free-radical emulsion polymerization. At the beginning of each copolymerization, the reactor was charged with a seed latex containing 50 g of PS and the amount of distilled water required to complete 1,200 g of water. Then, 10 sequential "monomer feeding stages" of 12 min each one were implemented following one of the four different feeding profiles, as shown in Figure 1. At the beginning of each stage, an aqueous solution containing 50 g of water, 0.9 g of APS, and 0.9 g of SDS was added as a shot, followed by the direct addition of an aqueous solution containing 30 g of water with 0.9 g SB to start the reaction. For every stage, the amount of APS, SB, and SDS was 2 wt% with respect to the total monomer mass to be added in each stage. The recipes for the synthesis of all the different polymeric materials are collected in Table 1.

2.3 Molecular weight measurement.

Number-average molecular weight (M_n) and weight-average molecular weight (M_w) of the polymeric materials were measured by size exclusion chromatography, using as solvent dimethylformamide containing 0.1% LiBr as eluent at 50°C (DMF, Scharlau GPC grade); 5 mg of sample in 1 mL of DMF were used in a Waters 1,515

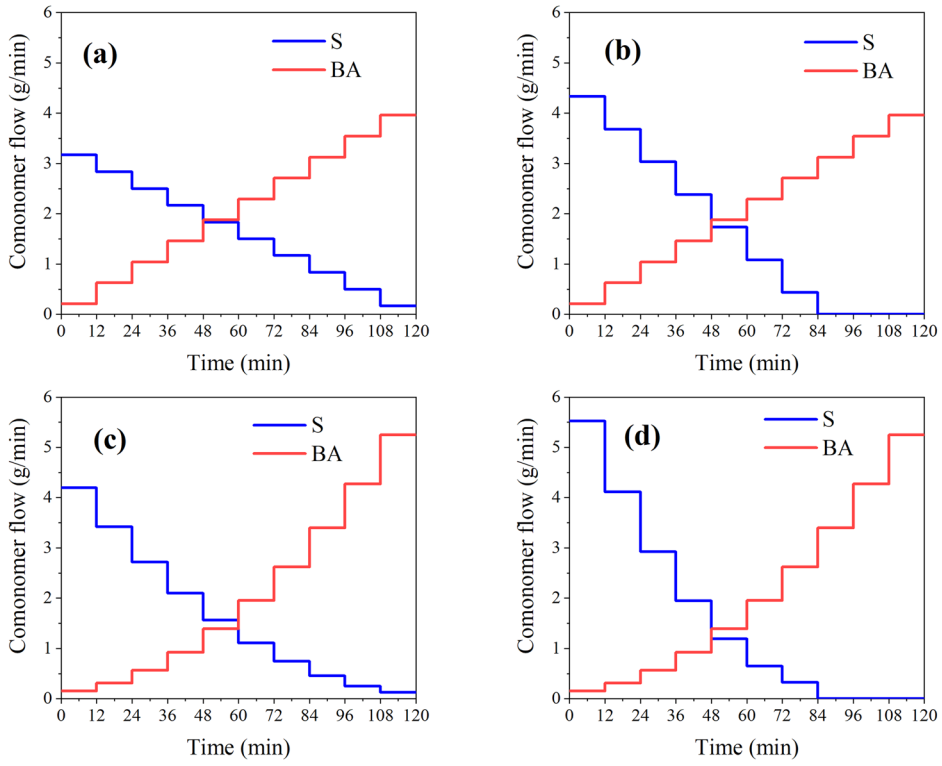

Figure 1: Feeding profiles for FCC: (a) linear–linear type 1 (GLL1), (b) linear–linear type 2 (GLL2), (c) parabolic–parabolic type 1 (GPP1), (d) parabolic–parabolic type 2 (GPP2).

Table 1: Mass content of the ingredients used for the synthesis of all polymeric materials

Components	PS Load added (g)	SC Load added (g)	FCC Load added (g)
Latex[a]	—	—	250.0
S	500.0	250.0	200.0
BA	—	250.0	250.0
SDS	10.0	10.0	9.0
KPS	10.0	—	—
Sb	10.0	—	—
APS	—	25.0	9.0
SB	—	25.0	9.0
Distilled water	2000.0	2000.0	2000.0

[a] The solid polymer content was 20 wt%.

chromatograph equipped with autosampler and refractive index detector (Waters model 410 refractive-index detector). Poly(methyl methacrylate) standards (4.8×10^5–1.90×10^3 g mol^{-1}) supplied by Polymer Laboratories Ltd, were used for the calibration.

2.4 Determination of copolymers composition by ^{1}H-NMR

To measure copolymer composition along with conversion, samples were extracted at the end of each feeding stage and at the end of the reaction. Samples were dried for gravimetric and composition measurements. Copolymer composition was determined using ^{1}H-NMR (JEOL 600 SS of 600 MHz), using a 5 mg sample in 1 mL of deuterated chloroform (Sigma-Aldrich).

2.5 Sample purification and processing

The latexes were dried in a chamber at ambient conditions, using airflow for drying. Afterward, the solid material was washed several times with distilled water and dried again in the chamber. Then, small polymeric fragments were obtained by manual cutting to be processed by compression molding (Carver Press model 3895) at 20.7 MPa using a 15 min cycle at 150°C for the process. The samples for mechanodynamic and tensile tests were,

respectively, molded in accordance with ASTM D 4065-01 and ASTM D 638-03.

2.6 Dynamic mechanical analysis (DMA)

Mechanodynamic tests as a function of temperature were performed in a dynamic mechanical analyzer (TA Instruments Q800) using a three-point bending clamp with an amplitude of 10 μm at 1 Hz and a heating rate of 1.5°C/min.

2.7 Tensile tests

Tensile tests were carried out at 23 ± 2°C using a temperature chamber and a crosshead speed of 5 mm/min with specimens type IV in a United SFM Electro-Mechanical Series Universal Testing Machine.

2.8 Hardness

Hardness was measured by means of a Shore A durometer (PTC instruments model 320) with rectangular specimens and conditions according to ASTM D 2240-00.

3 Results and discussion

For all the synthesized FCC, 45 min after the final feeding stage, the global conversion was >94%. Such situation confirms that the redox initiation is very convenient and shows that the materials were obtained in equivalent form. Another important factor to be able to validate the comparison of the mechanical properties has to do with their average molecular weights and molecular-weight dispersity ($Đ_M$). These values can be observed in Table 2, showing that the M_n and $Đ_M$ values confirm that the independence of mechanical properties with molecular weight can be stated. That is, the average M_n's are $>10^5$, and the $Đ_M$'s present reasonable values for semicontinuous reactions (26), which shows the stability of the system about the relation that exists between the comonomer mass flow and the generated radicals with the redox initiation system (which is also fed along conversion to maintain such relation). Besides, no gel formation was observed for the reactions, which sometimes occurs in redox emulsion polymerization reactions (27).

Table 2: Global conversion and molecular weights, of all polymeric materials and their molecular-weight dispersity. For FCC codes, see Figure 1

Polymeric material	Global conversion (%)	M_n ($\times 10^{-5}$) (Da)	M_w ($\times 10^{-5}$) (Da)	$Đ_M$
GPP1	100	1.29	2.74	2.12
GPP2	100	1.27	3.01	2.36
GLL1	100	1.41	3.34	2.37
GLL2	100	1.30	2.93	2.30
SC	94	1.18	2.72	2.30

The usefulness of WCD histograms to understand the mechanical behavior of copolymers has been demonstrated for copolymers of different global compositions using thermal initiators (10). Here, the improvement for the feeding profile–histogram relationship (looking for a close feed composition–copolymer composition relation) that can be obtained using redox initiators is shown presenting sequential composition histograms along with conversion for linear and parabolic feeding profiles. The WCD histogram of the SC (which is the reference material) is also presented. In Figure 2, the evolution of the histograms that come out as a result of the feeding procedures are presented. The comparative analysis of the final histograms for both types of feeding profiles with the respective histograms is discussed using Figures 2 and 3.

For the SC, since a batch reaction is used (without seed), the evolution of the histogram solely depends on the comonomer relative reactivities. There, at 25% conversion, the copolymer composition distribution is located in the 25–65% S region, indicating that for this redox system, the BA monomer reacts faster than S (28). As conversion advances to 50%, increments in the copolymer weight fraction (CWF) can be noticed within the same region, especially in the 35–60% S, still denoting higher conversion for BA. For 75% conversion, the increment in CWF is more noticeable in the 45–60% S region, indicating a higher conversion for the S monomer. For the final conversion, the remnant BA reacts with the existent S, showing also a very small fraction on the right side of the histogram, denoting that at the end of the reaction, the remaining reactant mixture is almost pure S.

For all of the FCC, the PS seed, which is part of the initial recipe charged to the reactor, appears in every histogram, representing 0.1 of the CWF in the 95–100% S bar. For the GLL1 (Figure 2b), the tendency to form chains that are richer in BA is very clear for the 0–25%

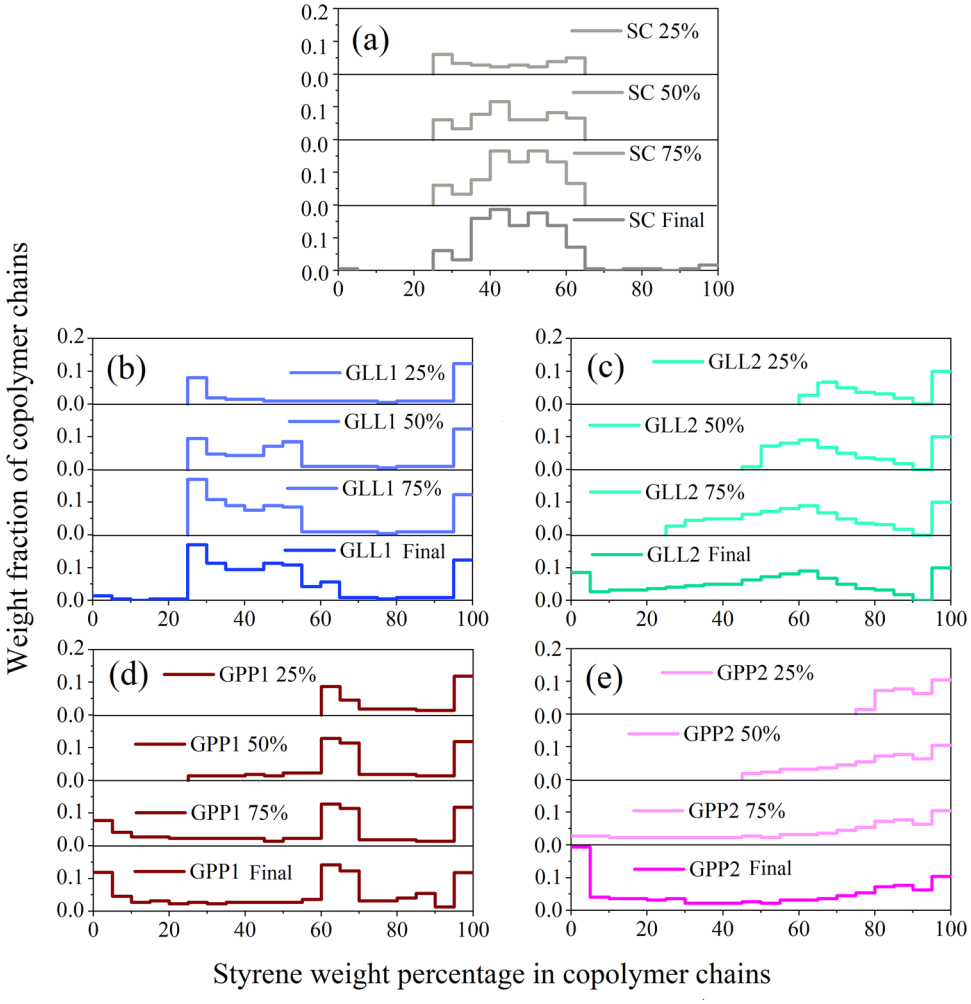

Figure 2: Evolution of the WCD for SC and FCC represented by histograms advance along with conversion. (a) SC, (b) GLL1, (c) GLL2, (d) GPP1, (e) GPP2. For FCC codes, see Figure 1.

conversion. In that way along with the column that mainly represents the PS seed (0.124 CWF), appears one column in the 25–30% S. Besides, a small number of chains is formed within the 30–95% S. At 50% conversion, there is a noticeable increment in the 25–55% S still denoting the higher BA reactivity, with some S increment in the copolymer chains associated with the accumulated S monomer. For the 75% conversion, the increment in chains fraction within the same region can be attributed to the increase in BA feed while for S is reduced, and such tendency continues for the final part of the reaction (75–100% conversion), although some chains fraction within the 55–65% region are also formed with the remnant S.

Observing the whole evolution of the GLL1 histogram first, and the evolution of the GLL2 histogram afterward, the operability of the FCC synthesis method (using redox initiation) to produce changes in the WCD along conversion (0–100%) is clearly shown (Figure 2c). At 25% conversion, the high S concentration in monomer feed allows the formation of chains in the 60–90% S region, and as the reaction advances, the WCD has expanded to 45% S at 50% conversion and to 25% S at 75% conversion, while showing some CWF increments in the 45–65% S region as the S monomer concentration decreases, while the concentration of BA increases. The remnant S along with the high BA concentration for the feed in the last part of the reaction, allow the formation of chains rich in BA, and even in the 0–5% S bar, showing one way with this chemical system to cover the WCD with linear profiles.

For the GPP1 material (Figure 2d), the parabolic feeding profile allows at the 25% conversion a considerable amount of chains formed in the 60–70% S region, along with small amounts for the 70–100% S zone. At 50% conversion, a small amount of chains is formed between 25% and 60% S, while the CWF for the 60–70%

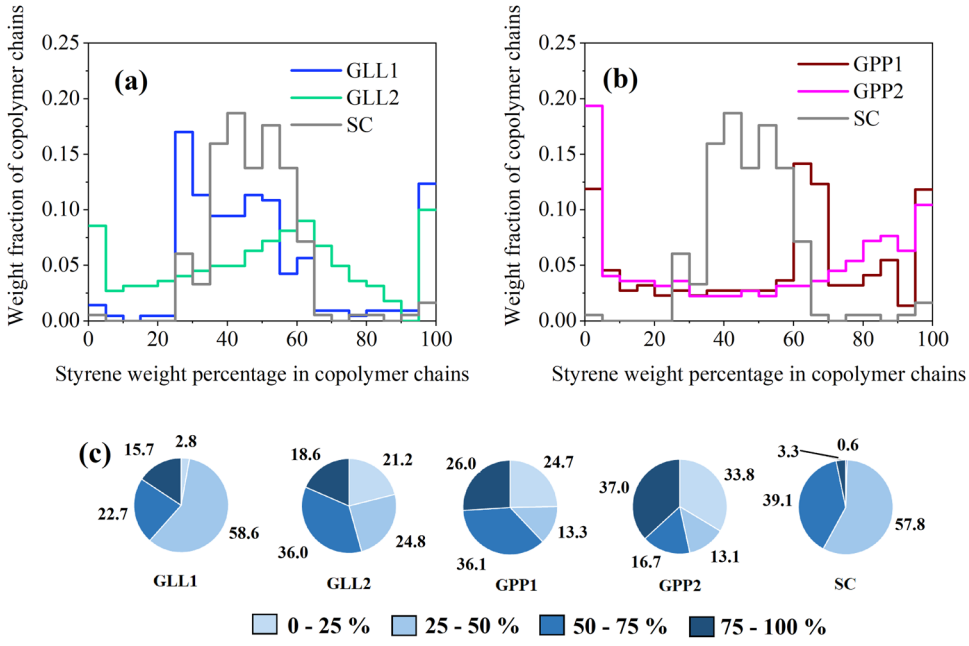

Figure 3: (a and b) WCD histograms of the SC and FCC: (a) SC, GLL1 ,and GLL2: (b) SC, GPP1, and GPP2; (c) mass percentage of copolymer chains at 25% intervals for all polymeric materials. For FCC codes, see Figure 1.

keeps growing. The CWF in the latter region continues increasing until the end of the reaction, while the chains rich in BA extend to 0–5% S at 75% conversion, and keep increasing especially in the 0–40% S for the 100% conversion, along with an increment in the 80–90% S attributed to the remnant S.

For the GPP2 material (Figure 2e), the forced fast S feeding allows the formation of chains in the 75–95% S for the 0–25% conversion. As the reaction advances to 50% conversion, the CWF extends to chains that contain more BA (45–80% S) and extends to the 0–45% S at 75% conversion (in a similar way to GLL2), with no increase in the 45–100% S. For the 100% conversion, a significant increment in the 0–25% S can be noticed (but especially in the 0–5% S bar), giving this profile to the histogram, in the end, an important CWF in the extremes of the spectrum.

The final WCD of the SC (synthesized using a batch process) has been included as a reference (along with the correspondent histograms of the FCC) to show the reasoning behind the mechanical properties that come out for the copolymer that is made depending on its comonomer reactivities. In Figure 3a and b, for the SC it can be seen that 97% of the copolymer chains are between 25% and 65% S, denoting a small tendency to the left side of the histogram, basically containing more chains that are rich in BA. Moreover, for the 25–50% S region, there are 57.8% chains, while for the 50–75% S, there are only 39.1% chains (Figure 3c). That is a result of the higher preference that the redox pair shows for BA (28). This type of histogram would be reflected as one of a material with a low modulus and high deformation capacity.

In the semicontinuous reaction system implemented for the FCC, using linear–linear profiles, if the monomers flow is close to relatively equilibrated comonomers mass feed, there would be the possibility to obtain a WCD resembling that of the SC if the redox reaction contributes to avoid excessive monomer(s) accumulation in the reaction locus. For the GLL1 system, such type of feeding profile (Figure 1a) leads to a histogram that is close to the one obtained for the SC (Figure 3a). About 58.6% of the copolymer chains appears on the 25–50% S region, while 22.7% and 15.7% appear, respectively, in the 50–75% and 75–100% S, highly promoting elasticity, as in the SC case. Under such circumstances, to promote chains formation with higher S content, for GLL2, S was fed faster with respect to BA (Figure 1b). In that way, a close to equilibrated histogram for chain composition was obtained (Figure 3a). For the 0–50% S, 46% of chains appear in Figure 3c, showing in addition, 21.2% and 18.6% respectively in the 0–25% S and 75–100% S. It is clear that with respect to the former materials (SC and GLL1), higher moduli can be expected, along with considerable deformation.

To look for alternated high monomer concentration over the copolymer composition regions that are rich in S or rich in BA, parabolic–parabolic feed profiles were used

to form copolymer chains with such characteristics (i.e., rich in S in the first stages and rich in BA in the last feeding stages). Looking at Figure 1c and d, for the parabolic profiles, the basic difference between them is similar to the difference between 1a and 1b; that is, there would be more tendency to form chains for middle compositions with GPP1, while for GPP2, copolymer chains with richer concentrations on the extremes of the WCD could be expected (referred to GPP1). Important differences occur in the 0–5% bar and the 60–95% S region.

Looking at Figure 3c, as a basic perspective, considering the higher rubbery regions (0–50% S) and the more rigid zones (50–100% S), the Young modulus values at environmental conditions would present the following ascendant order (considering that for nearby values for the materials within the 50–100% S zone, the section with more importance for the modulus contribution is the 75–100% S): GLL1, SC, GLL2, GPP2, and GPP1.

Since the mechanical properties depend on the WCD, the histograms allow the understanding of the behavior for the SC, the FCC, and their comparison. The similarity in histograms for SC and GLL1, will take them to a close mechanical behavior; although according to their differences described in the discussion of Figure 3a, the GLL1 will show a "rubberier" behavior, while the other FCC would show higher elastic modulus.

Looking at Figure 4a, for the very low-temperature region (from −60°C to −40°C), all polymeric materials show a high similar storage modulus (E') value. However, for GPP1 and GPP2, it started to decrease first, and at −10°C, the curves are clearly below the ones of the other materials. That situation is basically related to the number of chains (rich in BA) that they contain in the 0–20% S. The GLL2 is the next one following such behavior, due to the same reason. The GLL1 material stays closer to the SC material in the whole trajectory, showing an E' decay with a small inclination, denoting an approximation to a weighted glass transition temperature (T_g) value. The non-vertical E' decays apply to the rest of the FCC (GLL2, GPP1, and GPP2). These materials present a significant amount of chains in the 65–100% S, and looking at Figure 3c, it can be noticed that the higher the amount of CWF in the 75–100% S region, the higher the temperature required for the E' final decay.

For the loss modulus (E'') behavior (Figure 4b), the wider the chain's composition within the histograms, the broader the main peak(s) related to the T_g(s) of the materials. At approximately −30°C, the variation in E'' for the FCC is related to the inclined trajectory in E', showing the presence of chains whose T_g is around that value, and the higher the number of chains with such composition, the higher the peak that appears in E''. In that way, the lowest peak for the FCC at that temperature corresponds to GLL1, and the highest to GPP2. That is in accordance with the CWF in the 0–25% S region, which is shown in Figure 3c. In relation to the main peak of the materials that show one clear peak above 0°C, the rank in ascendant order is GPP1, GLL2, GLL1, and SC (peak at 30°C). With respect to GPP2, looking at the very wide peak from −40°C to approximately 10°C, two crests may be mentioned at −25°C and 0°C. These crests (denoting T_g's) are related to the respective CWF in the 0–25 and 25–50 regions (Figure 3c). Besides these crests, a "tail" from 40°C to 83°C, which is in accordance with the extension in E', can also be noticed. Such uncommon behavior can be explained by its low WCF content in the 5–70% S region, which promotes phase separation. Nevertheless, it presents the highest energy dissipation capacity for the −40°C to 0°C range and still holds some E′ and E″ values for the 40–80°C temperature range. For the comparison of the energy dissipation capacity from −40°C to 40°C shown in Table 3, it can be noticed that the SC and GLL1 hold the

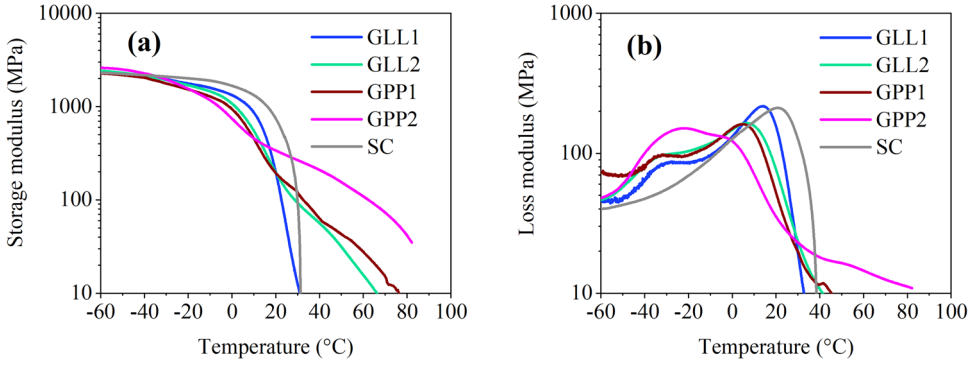

Figure 4: (a) Storage and (b) loss moduli as a function of temperature for the different polymeric materials, with a ramp rate of 1.5°C/min and frequency of 1 Hz. For FCC codes, see Figure 1.

Table 3: Weight percent composition, Young and storage moduli, ultimate stress and strain, and energy dissipation capacity (from –40°C to 40°C) of the different polymeric materials. For FCC codes, see Figure 1

Property	GLL1	GLL2	GPP1	GPP2	SC
Weight percent composition (S/BA, %/%)	49.7/50.3	49.2/50.8	50.6/49.4	48.8/51.2	49.2/50.8
Young modulus (MPa)	0.5 ± 0.1	11.0 ± 0.9	39.7 ± 6.3	33.9 ± 1.6	2.2 ± 0.4
Ultimate stress (MPa)	1.0 ± 0.3	2.0 ± 0.2	2.3 ± 0.1	2.8 ± 0.2	1.6 ± 0.3
Ultimate strain (%)	2,397 ± 75	680 ± 67	279 ± 26	88 ± 9	2,073 ± 115.1
Energy dissipation capacity (MPa)	8,129	7,762	7,234	7,419	8,824

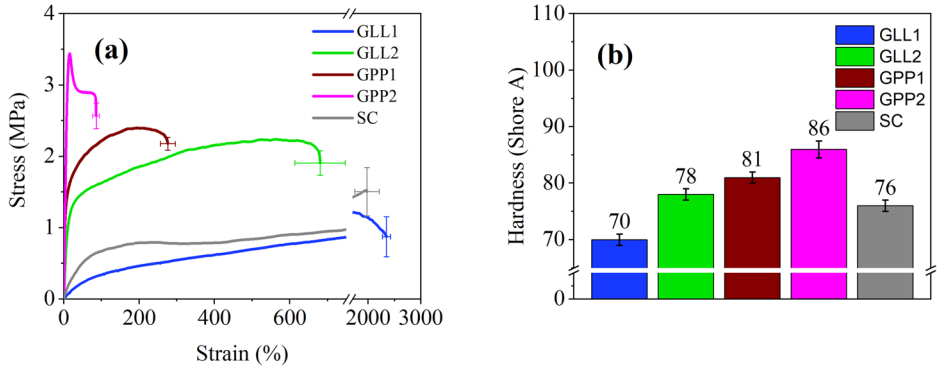

Figure 5: (a) Stress–strain and (b) shore A hardness behavior of the different polymeric materials at 25 ± 2°C. For FCC codes, see Figure 1.

higher values. Nevertheless, the other materials can still hold high energy dissipation within the temperature range of the study, due to their dissipation capacity in the low-temperature range, which is low for the SC material.

From the stress–strain properties shown in Figure 5 and Table 3, it can be seen that the Young's moduli and deformation capacity follow the trend similarity for SC and GLL1 of Figure 3a. The slight differences are due to the minor shift to the left for GLL1 (in the 15–35% S region of Figure 3a), leading to smaller modulus but higher deformation. The GLL2 material shows an equilibrated histogram, combining an increase in modulus and considerable deformation capacity (with respect to GLL1). The completely covered "pyramid" formed by chains within the 5–95% S (with a peak at 60–65% S), with columns on both sides, validating such behavior and properties combination. For the GPP1 and GPP2 materials, the histograms show similarity from 0–55% S; although for the 0–5% S bar, the high CWF for GPP2 contributes to lack of chains interaction because the CWF content is low between 10 and 70% S. The differences in the 55–95% S for GPP1 and GPP2 are closely compensated for their contribution to the modulus. For the 55–70% S, the CWF of GPP1 is noticeably higher, but in the 70–95% S, there is a converse relation (with chains very rich in S, that have high influence in modulus). In the end, the modulus for both is high, but for deformation, the GPP1 presents 279%, while the GPP2 shows only 88%. The high CWF content of chains rich in S contributes to their modulus, and the interaction for deformation is lower for the GPP2. An additional remarkable point of interest is related to the GPP2 whose glass transitions are considerably lower than that of the SC material (–25°C and 0°C vs 22°C), but its modulus is 15.4 times higher (Table 3). Such synergism is possible for the GPP2, because it contains enough amount of chains rich in S (especially in the 75–100% S region), showing also the highest yielding stress. The results obtained with the FCC demonstrate that using this method, by histogram tuning the moduli-deformation relationship can be optimized, and that elastomeric thermoplastics can be prepared (i.e. optimizing the histograms of the FCC discussed here).

For hardness, the behavior is aligned with the Young's modulus of the polymeric materials, except for GPP1 and GPP2. Nevertheless, for the stress–strain test, the values of GPP1 and GPP2 are statistically equivalent; besides, for this type of material, there is a difference between the two types of tests. For the tensile test, the interaction of the chain contributes to load support when the stress is applied, while for hardness the penetration in one point, does not allow the full chain interaction. In this case, by the high CWF content in the 75–100% S (Figure 3b), GPP2 shows a higher hardness value.

4 Conclusions

Following the WCD evolution of diverse FCC obtained with redox initiation reactions, it has been demonstrated that it is easy to promote desired changes in the WCD with specific purposes to modify copolymer properties with the same global composition.

Since there is a similarity in molecular-weight dispersity obtained using different mass flows for the reactions, it is clear that the method can be used consistently for different WCD's and global compositions.

The use of redox reactions to obtain FCC with low molecular-weight dispersity in short times and low temperature can be used to get a wide variety of WCD's, looking for synergism in properties for plastics or elastomers. Considering the low reaction temperature and short time for copolymer synthesis, this methodology is very attractive for industrial applications and can be applied immediately for polymeric materials with no limitations in molecular weight (i.e. the molecular weight can be controlled by simple stoichiometry as in any free-radical emulsion polymerization).

Acknowledgments: José Manuel Sandoval-Díaz thanks CONACyT for the scholarship during the Ph.D. program and Universidad de Guadalajara and Institute of Polymer Science and Technology, ICTP-CSIC, for the support to carry out part of the experimental research Luis Javier González-Ortiz for assistance in data analysis.

References

(1) Jakubowski W, Juhari A, Best A, Koynov K, Pakula T, Matyjaszewski K. Comparison of thermomechanical properties of statistical, gradient and block copolymers of isobornyl acrylate and *n*-butyl acrylate with various acrylate homopolymers. Polymer. 2008;49:1567–78.

(2) Morais V, Encinar M, Prolongo MG, Rubio RG. Dynamical mechanical behavior of copolymers made of styrene and methyl methacrylate: Random, alternate and diblock copolymers. Polymer. 2006;47:2349–56.

(3) Yoshida T, Kanaoka S, Watanabe H, Aoshima S. Stimuli-responsive reversible physical networks. II. Design and properties of homogeneous physical networks consisting of periodic copolymers synthesized by living cationic polymerization. J Polym Sci A Polym Chem. 2005;43: 2712–22.

(4) Odian G. Chain Copolymerization in Principles of Polymerization. vol. 6, 4th ed. New York, NY, USA: Wiley-Interscience; 2004. p. 464–543.

(5) Rudin A, Choi P. Free-Radical Polymerization in The Elements of Polymer Science & Engineering. 3rd ed. Oxford UK: Elsevier Inc.; 2013. p. 341–89.

(6) Allcock HR, Lampe FW. Contemporary Polymer Chemistry. 2nd ed. Englewood, NJ, USA: Prentice Hall; 1990.

(7) Gum WF, Riese W, Ulrich H. Reaction Polymers: Chemistry, Technology, Applications, Markets. 1st ed. Munich, Germany: Hanser Publishers; 1992.

(8) Lipatov YS, Karabanova LV. Gradient interpenetrating polymer networks. J Mater Sci. 1995;30:6710–8.

(9) Jasso-Gastinel CF, Salamone JC, Editors. Gradient Polymers in Polymeric Materials Encyclopedia. vol. 4, Boca Raton, FL, USA: CRC Press; 1996. p. 2849–56.

(10) Arnez-Prado AH, Gonzalez-Ortiz LJ, Aranda-García FJ, Jasso-Gastinel CF. The variation of comonomers feeding profile to design the distribution of chains composition for the optimization of the mechanical properties in copolymer systems. e-Polymers. 2012;69:1–15.

(11) Matyjaszewski K, Ziegler MJ, Arehart SV, Greszta D, Pakula TJ. Gradient copolymers by atom transfer radical copolymerization. Phys Org Chem. 2000;13:775–86.

(12) Wang L, Broadbelt LJ. Explicit sequence of styrene/methyl methacrylate gradient copolymers synthesized by forced gradient copolymerization with nitroxide-mediated controlled radical polymerization. Macromolecules. 2009;42: 7961–8.

(13) Sun X, Luo Y, Wang R, Li B-G, Zhu S. Semibatch RAFT polymerization for producing ST/BA copolymers with controlled gradient composition profiles. AIChE J. 2008;54: 1073–87.

(14) Li X, Mastan E, Wang W-J, Li B-G, Zhu S. Progress in reactor engineering of controlled radical polymerization: A comprehensive review. React Chem Eng. 2016;1:23–59.

(15) Xie L, Liu Q, Luo Z-H. A multiscale CFD-PBM coupled model for the kinetics and liquid–liquid dispersion behavior in a suspension polymerization stirred tank. Chem Eng Res Des. 2018;130:1–17.

(16) Devlaminck DJG, Van-Steenberge PHM, Reyniers MF, D´hooge DR. Modeling of miniemulsion polymerization of styrene with macro-RAFT agents to theoretically compare slow fragmentation, ideal exchange and cross-termination cases. Polymers. 2019;11:1–28.

(17) Yang W, Xie D, Sheng X, Zhang X. Sequence distribution and cumulative composition of gradient latex particles synthesized by a power-feed technique. Ind Eng Chem Res. 2013;52: 13466–76.

(18) Rivera-Gálvez FJ, González-Ortiz LJ, López-Manchado MA, Hernández-Hernández ME, Jasso-Gastinel CF. A methodology towards mechanical properties optimization of three-component polymers by the gradual variation of feed composition in semi-continuous emulsion-free radical polymerization. Polymers-Basel. 2019;11:1–13.

(19) Hong-Ru L. Solution polymerization of acrylamide using potassium persulfate as an initiator: Kinetic studies, temperature and pH dependence. Eur Polym J. 2001;37:1507–10.

(20) Jasso-Gastinel CF, Lopez-Ureta LC, Gonzalez-Ortiz LJ, Reyes-Gonzalez I, Toral L-D, Manero-Brito O. Synthesis and characterization of styrene-butyl acrylate polymers, varying feed

composition in a semicontinuous emulsion process. J Appl Polym Sci. 2006;106:3964–71.
(21) Misra GS, Bajpai UDN. Redox polymerization. Prog Polym Sci. 1982;8:61–131.
(22) Sarac AS. Redox polymerization. Prog Polym Sci. 1999;24: 1149–204.
(23) Lamb DJ, Fellows CM, Gilbert RG. Radical entry mechanisms in redox-initiated emulsion polymerizations. Polymer. 2005;46: 7874–95.
(24) Chonde Y, Liu LJ, Krieger IM. Preparation and surface modification of poly(vinylbenzy1 chloride) latices. J Appl Polym Sci. 1980;25:2407–16.
(25) Fokou PA, Meier MAR. Use of a renewable and degradable monomer to study the temperature-dependent olefin isomerization during ADMET polymerizations. J Am Chem Soc. 2009;131(5):1664–5.
(26) El-Aasser MS, Makgawinata T, Vanderhoff JW, Pichot C. Batch and semicontinuous emulsion copolymerization of vinyl acetat–butyl acrylate. I. Bulk, surface, and colloidal properties of copolymer latexes. J Polym Sci A1. 1983;21:2363–82.
(27) Kohut-Svelko N, Pirri R, Asua JM, Leiza JR. Redox initiator systems for emulsion polymerization of acrylates. J Polym Sci Pol Chem. 2009;47:2917–27.
(28) Huang H, Zhang H, Li J, Cheng S, Hu F, Tan B. Miniemulsion copolymerization of styrene and butyl acrylate initiated by redox system at lower temperature-preparation and polymerization of miniemulsion. J Appl Polym Sci. 1998;68: 2029–39.